Integration of AFTA and (U-Th)/He thermochronology to enhance the resolution and precision of thermal history reconstruction in the Anglesea-1 well, Otway Basin, SE Australia

P.F. Green[1], P.V. Crowhurst[2] and I.R. Duddy[1]

Abstract

Apatite fission track analysis and vitrinite reflectance studies of the Otway Basin (Southeastern Australia) have revealed numerous mid-Cretaceous, mid-Tertiary and Late Tertiary tectono-thermal events, reflecting both temporal variation in basal heat flow and episodes of deeper burial and subsequent exhumation. In particular, results from the Anglesea-1 well reveal two dominant paleo-thermal episodes with cooling beginning from maximum paleotemperatures in the mid-Cretaceous and from a lower paleo-thermal peak in the Tertiary. The timing of this more recent cooling episode is relatively poorly defined, due to a combination of factors including the virtual absence of the more sensitive fluorine-rich apatites in samples from Early Cretaceous Otway Group volcanogenic sediments.

The unique low temperature sensitivity of apatite (U-Th)/He dating offers the potential to define the timing of this more recent cooling episode with greater precision. Using a thermal history framework provided by AFTA and VR data, comparison of modelled (U-Th)/He ages for a range of viable scenarios with measured ages allows refinement of the onset of Late Tertiary cooling to the interval 12–7 Ma. This timing correlates closely with a regional Late Miocene unconformity, long recognised but recently documented in some detail.

Integration of (U-Th)/He dating with AFTA and VR provides increased precision in the timing of low temperature paleo-thermal episodes, and in resulting thermal history reconstructions, in turn allowing improved definition of the thermal evolution of potential hydrocarbon source rocks. Application of these techniques can significantly reduce exploration risk by focussing on regions where hydrocarbon generation post-dates structuring.

Keywords: AFTA®, (U-Th)/He thermochronology, basin modelling, Anglesea-1, Otway Basin, Early Cretaceous heat flow, Neogene Tectonics, Miocene exhumation.

Introduction

Application of Apatite Fission Track Analysis (AFTA®) to define both the timing and magnitude of paleo-thermal episodes in sedimentary basins—that is, episodes in which the now preserved sedimentary section reached higher temperatures at some time in the past—is well established as a tool for hydrocarbon exploration (Argent et al. 2002; Duncan et al. 1998; Green et al. 2001a). By defining areas where the main phase of hydrocarbon generation post-dates the formation of potential trapping structures, application of AFTA, in tandem with complementary techniques such as vitrinite reflectance (VR), allows delineation of those areas where timing relationships are most favourable for the accumulation of hydrocarbons (e.g. Green et al. 1997; Duddy 1997; Duddy & Erout 2001; Duddy et al. 2003). The ability to define multiple episodes also allows information to be obtained on the likelihood of preservation of accumulated hydrocarbons to the present day (e.g. Green et al. 2001a).

Thermal history reconstruction, based on application of AFTA and VR, can also be useful in studying regional tectonics, in revealing and delineating episodes of basin inversion (e.g. Green et al. 1995), regional uplift and erosion (i.e. exhumation) (e.g. Green 2002) and heating due to hot fluid circulation (e.g. Duddy et al. 1994, 1998).

1. Geotrack International Pty Ltd., 37 Melville Rd., Brunswick West, VIC 3055, Australia.
2. CSIRO Petroleum Resources, PO Box 1130, Bentley, WA 6102, Australia.

Previous application of these techniques to the Otway Basin of Southeastern Australia has revealed a number of tectono-thermal events, including mid-Cretaceous, mid-Tertiary and Late Tertiary episodes, reflecting both temporal variation in basal heat flow and episodes of deeper burial and subsequent exhumation (Duddy 1994, 1997; Duddy & Erout 2001; Duddy et al. 2003). In particular, Duddy (1994) reported that AFTA data in the Anglesea-1 well reveal two dominant paleo-thermal episodes with cooling beginning from maximum paleotemperatures in the mid-Cretaceous (100 to 95 Ma), and from a subsequent paleo-thermal peak of lesser magnitude in post-Eocene times. As will be explained in more detail in the following, the relatively broad timing constraint for the more recent cooling episode is due to a combination of practical factors, including the virtual absence of the more sensitive fluorine-rich apatites in samples from the Early Cretaceous Otway Group volcanogenic sediments.

The unique low temperature sensitivity of the relatively new thermochronological technique of apatite (U-Th)/He dating offers the potential of improved precision on lower temperature events. Particularly when integrated with information from AFTA and other thermal indicators (e.g. VR), this technique can allow more precise thermal history constraints to be established at relatively low temperatures in the range 50 to 80ºC (e.g. Crowhurst et al. 2002). In this study, we have set out to establish tighter constraints on the more recent cooling episode defined from AFTA in the Anglesea-1 well, by integrating published apatite (U-Th)/He ages with the thermal history framework provided by new AFTA and VR data.

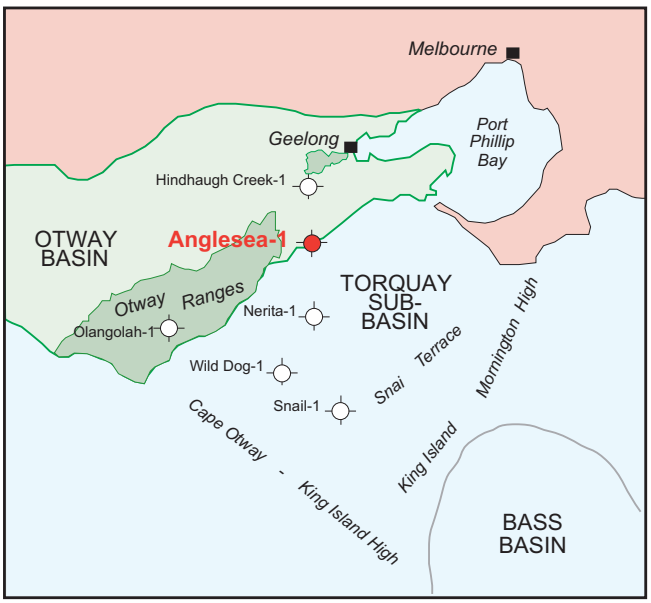

Figure 1. Location map showing the Otway Basin, basic tectonic elements and the location of the Anglesea-1 well discussed in this paper.

Geological setting of the Anglesea-1 well and previous thermal history studies

The Anglesea-1 well is located within the onshore eastern Otway Basin, one of a series of basins formed during rifting of the southern margin of Australia (Fig. 1). Volcanogenic sediments of the Otway Group are overlain by siliciclastic Late Cretaceous units of the Sherbrook Group, while siliciclastic and carbonate Tertiary units are divided into the Wangerrip, Nirranda and Heytsbury Groups. An angular unconformity occurs at the top of the Otway Group at some locations, and additional unconformities occur at various intervals within the Tertiary section, recording a complex and varied tectonic history. For further details, see e.g. Trupp et al. (1994); Duddy (1994, 1997); Cooper (1995); Cooper & Hill (1997); Geary et al. (2001).

Duddy (1994) reported results of an earlier AFTA study of samples from the Anglesea-1 well, which he interpreted as revealing two episodes of cooling from elevated paleotemperatures: an earlier episode in which cooling began between 95 and 100 Ma, and a later episode involving cooling from lower peak paleotemperatures, which began in post-Eocene time. Based on paleogeothermal gradients indicated by VR data from the well, Duddy (1994) interpreted the earlier episode as representing a combination of deeper burial and elevated heat flow, while the more recent episode could be explained by burial alone. Cooper & Hill (1997) reported similar conclusions based on their study of the well.

House et al. (1999) reported (U-Th)/He ages in apatites from a series of samples taken from Otway Basin hydrocarbon exploration wells, in a study aimed at defining the temperature sensitivity of the technique in geological conditions. They showed that measured ages, while showing considerable scatter, were progressively reduced at present-day temperatures in excess of approximately 40ºC, and were totally reset at temperatures around 80ºC. By comparing measured ages with values predicted on the basis of laboratory diffusion systematics and published thermal histories, they found generally good agreement in wells from the east of the basin. House et al. (2002) further investigated these data and results from additional wells in the region, and showed that much of the scatter in measured ages could be attributed to the role of grain size in controlling He diffusion systematics (Farley 2000; Reiners & Farley 2001).

House et al. (1999) calculated thermal histories for samples from the Anglesea-1 well based on the reconstruction reported by Duddy (1994) which showed cooling in the most recent episode beginning at approximately 40 Ma. But Duddy (1994) reported that AFTA data in this well only constrained cooling to post-Eocene, with a range of solutions being capable of explaining the data, only one of which was schematically illustrated (and subsequently being selected as a unique solution by House et al. 1999). In fact, Duddy (1994) speculated that a post-Middle Miocene timing may be more appropriate, this view being supported by Cooper & Hill (1997) who suggested a Middle Miocene-Pliocene timing. This uncertainty regarding the timing of the more recent cooling episode is one of the motivations for the present study.

Thermal history reconstruction tools

Thermal history reconstruction based on AFTA and VR data

To construct an initial thermal history framework within which the (U-Th)/He ages can be incorporated, we have used Thermal History Reconstruction based on application of Apatite Fission Track Analysis (AFTA) and vitrinite reflectance (VR) data. Using this approach, it is possible to identify the timing of dominant episodes of heating and cooling that have affected a sedimentary section, to quantify the variation of paleotemperatures through the section, and characterize mechanisms of heating and cooling (e.g. Bray et al. 1992; Green et al. 1995).

The variation of paleotemperatures with depth, or the "paleotemperature profile", provides key information on likely mechanisms of heating and cooling (Duddy et al. 1994; Green et al. 2002). Analysis is based on the assumption that heterogeneities in lithology through the section are sufficient to smooth out any potential large scale variations in thermal conductivity, so that variation of temperature with depth can be represented by a linear profile —this can be confirmed directly if BHT values are available at several depths through a well. On this basis, heating due solely to deeper burial should produce a more or less linear paleotemperature profile with a similar gradient to the present temperature profile. In contrast, heating due primarily to increased basal heat flow—perhaps also with a minor component of deeper burial—should produce a more or less linear paleotemperature profile with a higher gradient than the present temperature profile. Non-linear profiles are diagnostic of lateral introduction of heat, perhaps by hot fluid circulation.

Where heating can be attributed to deeper burial and/or elevated heat flow, fitting a linear profile to paleotemperatures as a function of depth allows the palaeogeothermal gradient at the paleo-thermal maximum to be determined, and extrapolation of the palaeogeothermal gradient from the depth of the appropriate unconformity to an assumed palaeo-surface temperature provides an estimate of the amount of section removed during cooling (Bray et al. 1992; Duddy et al. 1994; Green et al. 2002). This information allows the thermal history of all units within the sedimentary section to be reconstructed within a framework constrained by measured data.

Apatite Fission Track Analysis

AFTA (Green et al. 1989a) depends on analysis of radiation damage features ("fission tracks") within detrital apatite grains separated from sandstones and other clastic rock types. Fission tracks are generated continuously through time by spontaneous fission of uranium atoms, present within the apatite lattice at ppm levels, and are revealed in a polished surface by etching with dilute

acid. This provides the basis for determination of a fission track age which, in the absence of other effects, would measure the time over which tracks have accumulated in an apatite crystal. But in practice, while tracks are formed with an initial length within a narrow range, they shorten as a result of the repair of the radiation damage (known as "annealing") at a rate which depends on the prevailing temperature. Thus, as the temperature of a sample increases, tracks become shorter.

This process is irreversible, and if the temperature then drops, all tracks are effectively "frozen" at the length attained at the maximum temperature. Tracks which form after cooling are longer, due to the lower temperatures. Thus the proportion of short to long tracks measured in an apatite at the present-day reflects the time of cooling, while the mean length of the shorter component of tracks reflects the maximum paleotemperature. The fission track age is also reduced as a result of the track length reduction, due to the reduced probability that tracks can intersect a polished surface.

At a critical paleotemperature, "total annealing" occurs (i.e. the damage constituting the tracks is totally repaired, and track length is reduced to zero). The precise temperature where this occurs depends on the heating rate and the Cl content of the apatites. In samples which reached higher paleotemperatures, tracks are only retained after cooling below this limit. AFTA data from such samples provide only a minimum estimate of the maximum paleotemperature, but typically provide good constraints on the timing of the cooling episode. The annealing kinetics of fission tracks in apatite depends on the chlorine content of the apatite grains (Green et al. 1986). Incorporation of this variation in Cl content within each sample is essential in extracting correct thermal history information from AFTA data (e.g. Argent et al. 2002; Crowhurst et al. 2002; Green 2004).

Vitrinite reflectance

Vitrinite reflectance is based on the increasing reflectance of organic macerals with increasing temperature, and is commonly used in hydrocarbon exploration as an indicator of thermal maturity (e.g. Tissot & Welte 1984). VR data can be used to provide independent estimates of maximum paleotemperatures, through knowledge of the kinetics of the process. Such information constitutes a useful complement to the information derived from AFTA. A VR value of 0.7% corresponds closely to total annealing of fission tracks in apatite (Duddy et al. 1994).

In recent years it has become apparent that VR data generated by different analysts are not equivalent (discussion in Green et al. 2002). Approaches to VR analysis can be divided broadly into two types. We have found a high degree of consistency between thermal history interpretations from AFTA and VR data generated using an approach (Cook 1982) involving measurement of maximum reflectance under oil ($R_o$max) in polished thick sections, with identification of the indigenous vitrinite population being made on textural grounds, which allows an independent assessment to be made of the possible presence of reworked vitrinite populations from petrographic evidence, as well as allowing identification of caved material in sub-surface samples. Alternation between reflectance and fluorescence modes allows checking for associated fluorescing liptinite, bitumen impregnation, or the presence, intensity, and source of oil-cut which may affect the reading. The data presented here were generated in this way, which is the approach recommended by the International Commission on Organic and Coal Petrography. Many years experience with inter-laboratory comparisons has shown that consistent results can be obtained by different analysts (see the web site at www.iccop.org for further information).

An alternative approach, often encountered in hydrocarbon industry reports, involves measurements of random reflectance ($R_o$rand) in strewn slides of organic concentrates, with the indigenous vitrinite population often identified only by inspection of histograms of measurements and separation into perceived sub-populations. The inherent difference between $R_o$max and $R_o$rand arises because the reflectance of vitrinite is anisotropic (Cook et al. 1972), becoming increasingly so with increasing reflectance. Direct comparisons of these two measurements (Ting 1978; Zhang & Davis 1993) suggest that differences should be less than 10% (proportionally) for reflectances of 1% or less, but experience has shown that the two approaches can result in much larger differences in mean values, around 0.2% in absolute terms for values up to 1% (i.e. 0.8% $R_o$max cf. 0.6% $R_o$rand), which appear to be due to differences in analytical technique.

Therefore, in converting VR data to maximum paleotemperatures (see below) it is essential that the kinetic model used should be appropriate to the analytical approach. Experience in a variety of different settings suggests that the former approach described above, based on $R_o$max, yields estimates of maximum paleotemperature that are highly consistent with those from AFTA, if the Burnham & Sweeney (1989) algorithm for the kinetic response of VR is used. In contrast, VR data generated using the latter approach does not give consistent results using this method.

One important consideration, in the light of these comments, is that in assembling VR data for databases, it is essential that the method by which the data have been generated is also recorded, otherwise the values in isolation are ambiguous, at best.

Extracting thermal history information from AFTA and VR data

Both AFTA and VR data are dominated by maximum temperature. For this reason, extraction of thermal history information from AFTA and VR data begins by constructing a “Default Thermal History”, by combining the burial history derived from the preserved sedimentary section with the present-day geothermal gradient. If the measured data are consistent with the values predicted from this history, then the sample is presently at or close to its maximum post-depositional temperature, and the data retain little or no information on any palaeo-thermal effects. If, however, the data show a greater degree of fission track annealing or VR maturity than expected on the basis of the default history, the sample must have been hotter in the past. In this case, AFTA can provide an estimate of the time at which cooling began, and both AFTA and VR can define the magnitude of the maximum palaeotemperature reached by individual samples.

Extraction of thermal history solutions from AFTA and VR data is based on detailed knowledge of the kinetic responses of both systems which are calibrated from studies in both geological and laboratory conditions. Thermal history information is extracted from AFTA data by modelling the AFTA parameters—fission track age and track length distributions—expected from a variety of possible thermal history scenarios, and comparing the results with the measured data. By varying the magnitude and timing of the maximum paleotemperature employed in the modelling, the range of values of these parameters which give predictions consistent with the measured data, within 95% confidence limits, can be rigorously defined.

The basics of this modelling procedure are well established for mono-compositional apatites (e.g. Green et al. 1989b), based on a series of laboratory experiments on Durango apatite (Green et al. 1986; Laslett et al. 1987; Duddy et al. 1988). However, the annealing kinetics of fission tracks in apatite are known to be affected by the chlorine content (Green et al. 1986). In the studies described here, thermal history solutions have been extracted from the AFTA data using a "multi-compositional" kinetic model which makes full quantitative allowance for the effect of Cl content on annealing rates of fission tracks in apatite (Green et al. 1996, 2002). This model is calibrated using a combination of laboratory and geological data from a variety of sedimentary basins around the world. Palaeotemperature estimates from AFTA are quoted as a

range and have an uncertainty of between ±5 and ±10°C.

Observed VR values are converted to maximum paleotemperatures using the kinetic model developed by Burnham & Sweeney (1989) and Sweeney & Burnham (1990). Information on the timing of these maximum paleotemperatures is provided by the AFTA data. Paleotemperature estimates derived from VR data are reported here as single values but probably have a precision between 5 and 10ºC (based on typical levels of scatter within the data). The kinetic response of vitrinite reflectance as described by Burnham & Sweeney (1989) is very similar to the fission track annealing kinetic model developed by Laslett et al. (1987) to describe the kinetics of fission track annealing in Durango apatite. Total fission track annealing in apatites with typical Cl content (between 0.0 and 0.5 wt% Cl) corresponds to a VR value of approximately 0.7% (Duddy et al. 1991, 1994), regardless of heating rate.

Unlike VR data, AFTA data also provide some control on the history after the onset of cooling from maximum paleotemperatures, from the annealing of tracks formed during this period. Wherever possible, AFTA data from each sample are interpreted in terms of two episodes of heating and cooling, using assumed heating and cooling rates during each episode, with the maximum paleotemperature reached during the earlier episode. The timing of the onset of cooling and the peak paleotemperatures during the two episodes are varied systematically, and by comparing predicted and measured parameters the range of conditions which are compatible with the data can be defined. One additional episode during the cooling history is normally the limit of resolution from typical AFTA data, although in rare instances, data from a single sample can provide constraints on three discrete cooling episodes, if they are sufficiently separated in time and temperature (Green et al. 2001a).

Because AFTA and VR are dominated by maximum paleotemperature and preserve no information on the approach to the maximum, in order to extract thermal history solutions it is necessary to assume a value of heating rate. The precise value of maximum paleotemperature required to explain a particular set of data is sensitive to the assumed heating rate, and an order of magnitude change in heating rate is equivalent to a change of approximately 10ºC in the required paleotemperature (Green et al. 1989b).

It is important to stress that we do not attempt to constrain the whole thermal history of each sample from AFTA. Instead, we focus on those key aspects of the thermal history that control the development of the AFTA parameters—and VR values—specifically the maximum palaeotemperature of each sample and the time at which cooling from that palaeotemperature began, in one or two (rarely three) episodes.

Apatite (U-Th)/He dating

Apatite (U-Th)/He dating is a relatively new method of low-temperature thermochronology, based on the accumulation and diffusive loss of Helium produced by alpha decay of Uranium and Thorium impurities within apatite grains. Measurement of the amount of helium retained within an apatite grain, together with the uranium and thorium contents, allows calculation of a (U-Th)/He age (e.g. Zeitler et al. 1987; Lippolt et al. 1994; Wolf et al. 1996). Apatite (U-Th)/He ages are progressively reset by heating, due to the diffusive loss of the radiogenic helium, with total loss occurring at temperatures around 70 to 80ºC, for timescales involving millions of years (Wolf et al. 1998; Farley 2000). This diffusive loss is analogous to the "annealing" of fission tracks which leads to the shortening of fission tracks and resetting of apatite fission track ages at temperatures around 70 to 120ºC (Green et al. 1989a). Because of the low-temperature sensitivity of (U-Th)/He ages in apatite, the method has been successfully applied to a variety of geological problems (e.g. House et al. 1997; Wolf et al. 1997; Farley et al. 2001; Crowley et al. 2002).

While many of these studies involve application of (U-Th)/He dating in isolation, Crowhurst et al. (2002) demonstrated the particular strength of the technique when integrated with other methods of investigating thermal histories in sedimentary basins in samples from a hydrocarbon exploration well drilled on a major inversion structure in the Taranaki Basin, New Zealand. By

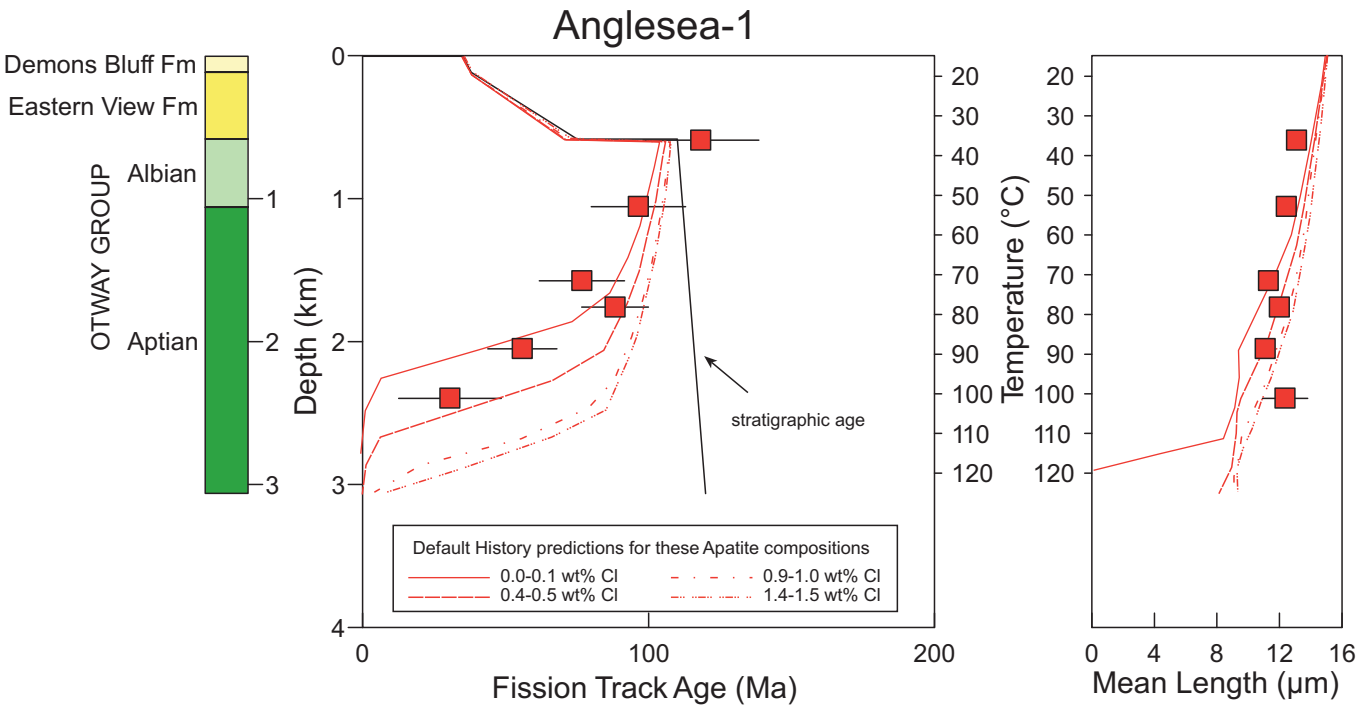

Figure 2. AFTA parameters plotted against sample depth and present temperature for samples from the Anglesea-1 well, Otway Basin, SE Australia. The variation of stratigraphic age with depth is also shown, as the solid line in the central panel. Present-day temperatures shown here are based on a surface temperature of 15ºC and a present-day thermal gradient of 36ºC/km, derived from corrected BHT data. Coloured lines show the pattern of fission track age and mean track length predicted (for apatites containing 0.0–0.1, 0.4–0.5, 0.9–1.0 and 1.5–1.6 wt% Cl) from the Default Thermal History, calculated as explained in the text.

combining the low temperature sensitivity of apatite (U-Th)/He dating with information at higher temperatures from AFTA, within a framework calibrated by VR, Crowhurst et al. (2002) demonstrated how the integrated dataset showed that cooling following the onset of Late Miocene inversion was protracted, probably involving two separate phases of inversion.

Results from the Anglesea-1 well

Geological information

The Anglesea-1 well was drilled in 1962 at a location near the foreshore in the Victorian coastal town of the same name (Fig. 1). The well intersected Late Cretaceous to Tertiary units of the Demons Bluff and Eastern View Formations, unconformably overlying Early Cretaceous units of the Otway Group, reaching TD at a depth of 3,065 m. Thus the section contains two major unconformities, representing the intervals 0 to 35 Ma and 75 to 110 Ma. Corrected BHT values (calculated using the approach described by Duddy et al. 2003), combined with a surface temperature of 15ºC, define a present-day thermal gradient of 36ºC/km.

AFTA data

Six samples of core, each of approximately 1 kg in weight, were processed from the Early Cretaceous Otway Group from depths between approximately 590 m and approximately 2,400 m. Sample details (depths, present-day temperatures) and results of fission track age and confined length measurements are summarised in Table 1. Fission track ages and mean track lengths

Table 1. AFTA and VR data and paleotemperature analysis summary for samples from Otway Basin well Anglesea-1

											Earlier event		Later event	
Sample Number	**Mean Depth (mkb)**	**Stratigraphic age[*1] (Ma)**	**Present temperature[*2] (ºC)**	**ρ_D[*3] (10^6 tracks /cm2)**	**ρ_s[*3] (10^6 tracks /cm2)**	**ρ_i[*3] (10^6 tracks /cm2)**	**Fission track age[*4] (Ma)**	**Mean track length (μm)**	**Standard levitation[*5] (μm)**	**VR (%)**	**Maximum paleotemperature[*6] (ºC)**	**Onset of cooling[*6] (Ma)**	**Maximum paleotemperature[*6] (ºC)**	**Onset of cooling[*6] (Ma)**
	152	38–75	20							0.34			53	
	243	38–75	24							0.34			53	
	335	38–75	27							0.42			70	
	545	38–75	35							0.42			70	
GC628–32	592	112–110	36	1.214 (1910)	0.921 (470)	1.916 (978)	118.3±10.1 (1%,20)	13.10±0.16	1.75 (115)		85–130	>55	60–80	55–5
	592	112–110	36							0.76	123			
	781	112–110	43							0.80	127			
	964	112–110	50							0.81	128			
GC628–33	1057	112–110	53	1.216 (1910)	0.313 (218)	0.770 (536)	96.5±8.3 (34%, 20)	12.44±0.18	1.82 (101)		>100 (>120	110–60 110-80)	60–90	65–0
	1224	120–112	59							0.96	140			
	1470	120–112	68							1.12	150			
GC628–34	1575	120–112	72	1.218 (1910)	0.293 (155)	0.908 (481)	76.7±7.4 (14%, 20)	11.30±0.20	1.99 (100)		>115 (>130	110–55 110-80)	90–110	60–5
RD63–34	1759	120–112	78	1.427 (2247)	0.417 (360)	1.273 (1099)	88.3±5.8 (44%, 20)	12.00±0.25	1.58 (40)		>100 (>130	>30 >90)	<110	70–0
	1759	120–112	78							1.35	163			
RD63–35	2050	120–112	89	1.428 (2247)	0.185 (109)	0.898 (528)	55.8±6.0 (19%, 20)	11.10±0.21	0.96 (22)		>115 (>130	100–40 100-60)	95–120	55–0
	2050	120–112	89							1.81	183			
	2300	120–112	98							2.41	205			
	2396	120–112	101							2.45	206			
RD63–36	2397	120–112	101	1.429 (2247)	0.169 (54)	1.530 (488)	30.5±9.0 (<0.1%	12.36±0.72	1.62 (5)		>110 (>130	105–0 105-60)	110–130	60–0
	2651	120–112	110							2.48	207			
	2941	120–112	121							3.23	232			
	3065	120–112	125							3.38	238			
											timing overlap[*7] (Ma):	**100–90**		**55–10**

[*1] All numerical values for stratigraphic ages assigned following Harland et al. (1989).

[*2] Present temperature estimates based on an assumed surface temperature of 15ºC, and a thermal gradient of 36ºC/km estimated from corrected BHT values.

[*2] ρ_S = spontaneous track density. ρ_i = induced track density. ρ_D = glass dosimeter track density. Numbers in parentheses show the number of tracks counted. Numbers in parentheses show the number of tracks counted in determining all track densities.

[*3] Values in parentheses denote P(χ^2) and number of grains analysed. Central age (Galbraith & Laslett 1993), used for samples containing a significant spread in single grain ages (P(χ^2)less than 5%). Ages were calculated using the zeta calibration approach of Hurford & Green (1983), using a zeta of 392.9 ± 7.4 (Analyst: Marilyn Moore) for samples GC628–32, –33 and –34, and 380.4 ± 5.7 (analyst C. O'Brien) for samples RD63–34, –35 and –36. All errors quoted at ± 1σ. All analytical details are as described by Green et al. (2001b), with the exception that thermal neutron irradiations showed a significant flux gradient, with the appropriate value of ρ_D for each sample determined by linear interpolation through the stack of grain mounts.

[*5] Numbers in parentheses show the number of track lengths measured.

[*6] Thermal history interpretation of AFTA data is based on an assumed heating rate of 1ºC/Ma and a cooling rate of 10ºC/Ma. Quoted ranges for paleotemperature and onset of cooling correspond to ±95% confidence limits allowed by the AFTA data (additional limits on the allowed time of cooling from higher paleotemperatures closer to the values indicated by VR data are shown in brackets for some samples).

[*7] A common timing for the onset of cooling in each episode can be assigned to all samples from the well, assuming that the paleo-thermal thermal effects identified in each sample represent synchronous cooling throughout the well. The latest constraint on the onset of cooling in the earlier episode is based in part on the maximum paleotemperature from VR, which the AFTA data show can only have been reached prior to 90 Ma.

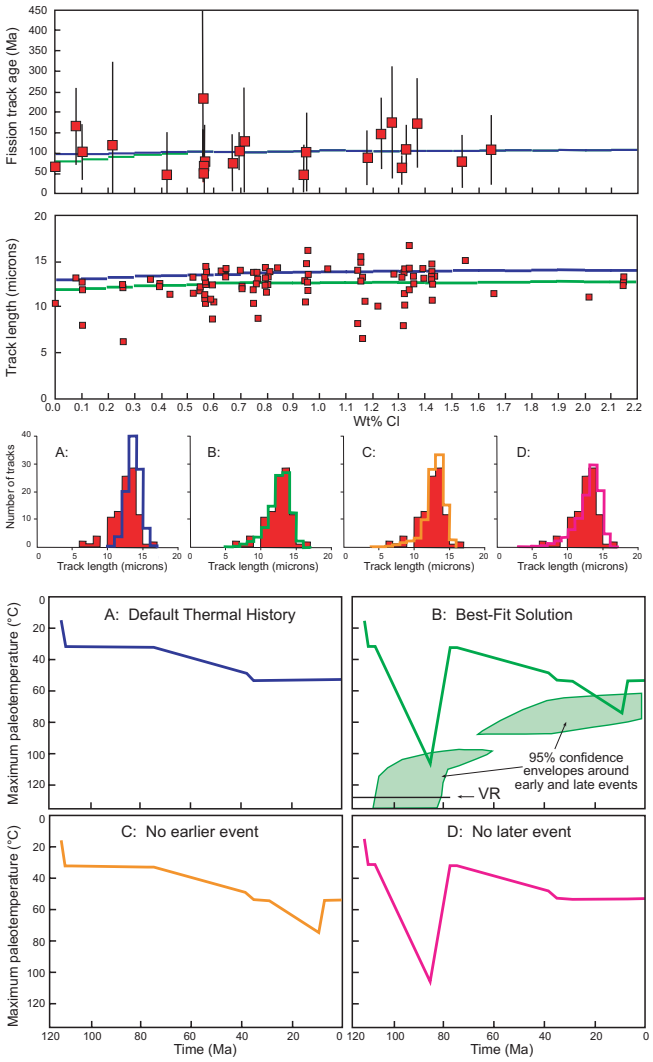

Figure 3. AFTA data in sample GC628–33, from a depth of 1,057 m in the Anglesea-1 well, illustrating the process by which thermal history information is extracted from the data. Upper plots show fission track ages of individual apatite grains and individual track lengths measurements within the sample, plotted against wt% Cl. The thick horizontal dashed lines in these plots show the trends of fission track age and mean track length vs Cl predicted from the Default Thermal History (blue) and from the best-fit history (green). Measured lengths are consistently less than the values predicted from the Default History, showing that this sample has been hotter in the past, although no significant age reduction is evident. The measured track length distribution in this sample is also shown (red histograms, central row), together with the distribution predicted from the Default Thermal History (A), the best-fit history (B), and versions of this history in which the earlier (C) or later (D) event has been removed. Clearly the length distribution predicted by the Default Thermal History provides a good fit to the observed distribution. Omitting the earlier event produces a predicted distribution in which the main mode is well reproduced but the fit is less good at lengths around 10 microns. Omitting the later event predicts more lengths around 10 microns but does not reproduce the main mode accurately. Only by including both episodes are all aspects of the track lengths distribution accurately reproduced. In detail, thermal history solutions are based on the distributions of track length within each compositional group (divisions of 0.1 wt% Cl width), rather than on the pooled distribution for the whole sample.

are plotted against sample depth in Figure 2, in which the variation of stratigraphic age with depth is also plotted. Trends of fission track age and mean length versus depth predicted from the Default Thermal History scenario (above) for the well are also shown, for various apatite compositions. Due to the wide spread in Cl contents in apatites from these samples, the interpretation of these data is not immediately apparent from Figure 2, and it is necessary to investigate the data within each sample in more detail, in order to reach firm conclusions regarding the extent of paleo-thermal effects in these samples.

Figure 3 illustrates the extraction of thermal history information from AFTA data, based on sample GC628–33, from a depth of 1,057 m and a present-day temperature of 53ºC. This example also highlights some of the subtleties and difficulties of the process. The trend of fission track age versus wt% Cl predicted from the Default Thermal History (DTH) is consistent with the measured ages, but the measured track lengths are consistently shorter than the values predicted from the DTH. This might suggest that while the sample has been hotter in the past, the maximum paleotemperature was not sufficient to produce significant age reduction. In fact such a conclusion is not accurate because VR data, to be discussed later, show that this sample has been heated to approximately 130ºC, sufficient to cause appreciable age reduction. But because cooling from this maximum paleotemperature began soon after deposition, the difference in timing is not resolvable within the data.

Using proprietary software that examines the degree of agreement between predicted and measured fission track age and track length as a function of chlorine content, for an input thermal history, a best-fit solution is defined on the basis of maximum likelihood theory (similar to that described by Gallagher 1995). The Default Thermal History is used as the starting point, with heating and cooling episodes superimposed, using assumed values of heating and cooling rate for reasons explained earlier. As also noted earlier, we do not attempt to constrain the entire thermal history, but focus on the maximum paleotemperature and the time at which cooling begins, in one or two episodes—as required to explain the data—as these are the prime factors which determine the AFTA parameters. Once the maximum likelihood values of maximum paleotemperature and time of cooling in each episode have been defined, 95% confidence regions around those values can be defined, also using likelihood theory.

In sample GC628–33, AFTA data require two discrete episodes of heating and cooling, in order to explain all facets of the AFTA data, as explained in Figure 3. Confidence regions around each episode are also illustrated in Figure 3. In similar fashion, AFTA data from the other five samples also require two episodes, and estimates of maximum or peak paleotemperature and the onset of cooling required to explain the AFTA data in each sample are summarised in Table 1. Note that the evidence for two episodes in sample GC628–33 is quite subtle, being derived from the detailed form of the track length distribution. More usually, evidence for multiple episodes might be provided by a severe degree of age reduction attained during the earlier episode while a more recent episode was revealed by shortening of the main mode of the track length distribution.

Two factors conspire to make interpretation of results from Anglesea-1 less straightforward than it might otherwise be. First, the onset of cooling from maximum paleotemperatures is relatively soon after deposition (see above, and later discussion). This makes it difficult to resolve the effect of cooling from high paleotemperatures from the start of the Default Thermal History (i.e. the depositional age) for each sample. Secondly, the samples from Anglesea-1 show a wide spread of Cl contents, reflecting their volcanogenic nature (Gleadow & Duddy 1981) and contain only a small proportion of the most thermally sensitive apatite grains with very low Cl contents (less than 0.3 wt% Cl). Most of the apatite grains, being more retentive than those more commonly encountered in most geological settings (e.g. Argent et al. 2002; Crowhurst et al. 2002; Green et al. 2002), have undergone relatively low degrees of fission track age reduction. Thus, evidence for multiple episodes can only be obtained from the details of the track length distribution in these more retentive apatites. Nevertheless, results from all six samples provide consistent interpretations, in terms of two discrete heating and cooling episodes.

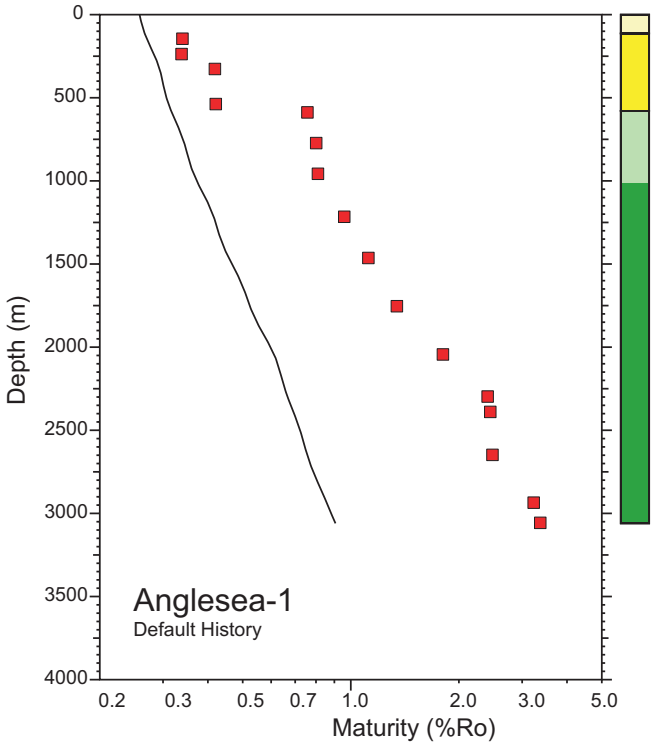

Figure 4. Vitrinite reflectance values in samples from the Anglesea-1 well, Otway Basin (summarised in Table 1), plotted against depth (from kb). The solid line shows the profile predicted from the Default Thermal History, that is, the history calculated from the assumption that all units throughout the well are currently at their maximum temperatures since deposition (see text). The Default Thermal History was constructed using the burial history derived from the section intersected in the well (shown in Fig. 5), combined with a present-day thermal gradient of 36ºC/km, derived from corrected BHT data and a surface temperature of 15ºC. All of the measured VR values plot above the profile, showing that the sampled units have been hotter in the past. A distinct break is evident across the Late Cretaceous-Eocene unconformity, suggesting a major difference in the magnitude of paleo-thermal effects across this unconformity.

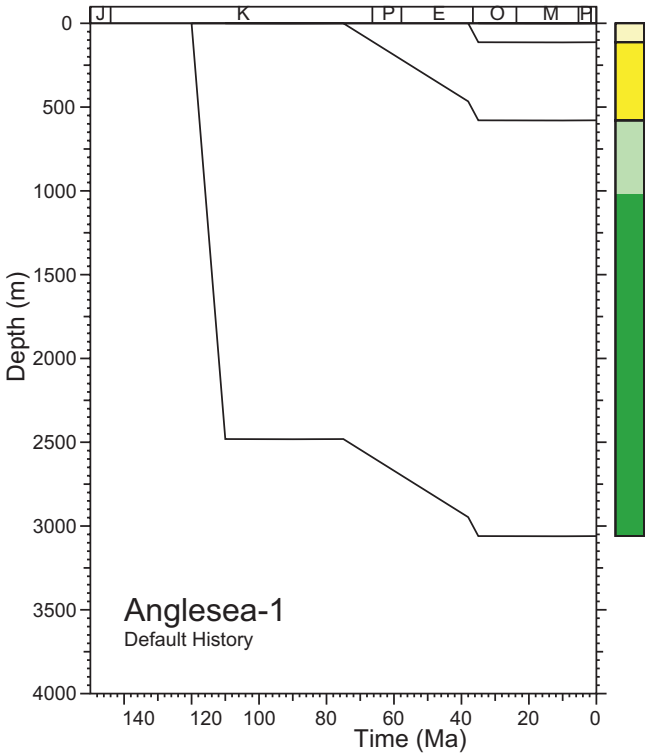

Figure 5. Burial History derived from the preserved section in the Anglesea-1 well, Otway Basin, used together with a present-day thermal gradient of 36ºC/km to predict Default Thermal Histories for individual samples and the profiles shown in Figs 2 and 4.

If we assume that results in each sample represent the effects of cooling which was synchronous throughout the sampled section, we can combine estimates of the onset of cooling from all samples to define the timing of the dominant cooling episodes. As summarised in Table 1, AFTA data in all samples analysed from the Anglesea-1 data can be explained in terms of an earliest episode of cooling from maximum paleotemperatures which began between 100 and 90 Ma, plus a later episode of cooling from lower peak paleotemperatures which began some time between 55 and 5 Ma. These timing estimates are consistent with earlier work (above), but provide no increase in precision over previous studies, largely due to the absence of low Cl grains as discussed earlier. Hence, the integration of apatite (U-Th)/He thermochronology offers significant potential rewards.

VR data

VR data in 16 samples from the Anglesea-1 well were taken from Open File data compiled by Constantine et al. (2001), and are summarised in Table 1. Four values are from samples of Tertiary age while the remaining samples are from the Early Cretaceous Otway group sediments. Mean values are plotted against depth in Figure 4, which also shows the VR-depth profile predicted on the basis of the Default Thermal History. The burial history used to construct the Default Thermal History, derived from the preserved sedimentary units intersected in the well, is shown in Figure 5. All of the measured VR values plot well above the profile predicted by the Default Thermal History in Figure 4, confirming the evidence from AFTA that the sampled units have been hotter in the past. Maximum paleotemperatures derived from the measured VR values, using the strategy outlined earlier, are summarised in Table 1. Maximum paleotemperatures from VR data in the Tertiary section are between 50 and 70ºC, increasing to 123ºC and higher in the underlying Early Cretaceous sediments.

Integration of thermal history interpretations from AFTA and VR

Paleotemperature constraints derived from AFTA and VR data are plotted against depth (from kb) in Figure 6. Comparison of paleotemperature constraints defined from AFTA in the shallowest sample, GC628–32, with those from VR data at the same depth shows that the maximum value defined from VR is consistent with the higher end of the range defined from AFTA for the earlier episode, while the range of paleotemperatures indicated by AFTA for the later episode is very similar to the maximum paleotemperatures indicated by VR from the overlying Tertiary section. Tertiary paleotemperature constraints derived from the AFTA data—which show that cooling began between 55 and 5 Ma—form a common array with maximum paleotemperatures from VR data in Tertiary units, and these are interpreted as representing the same event as recorded in the AFTA data. This being so, the stratigraphic age of the shallowest Tertiary unit suggests that cooling must have begun post–35 Ma, refining the timing of this more recent cooling episode to the interval 35 to 5 Ma. Similarly, the maximum paleotemperatures for the earlier episode derived from the AFTA data in the remaining five samples are highly consistent with those from the VR data in samples from Early Cretaceous units, and these VR data are therefore identified as representing a paleo-thermal maximum from which cooling began some time between 100 and 90 Ma.

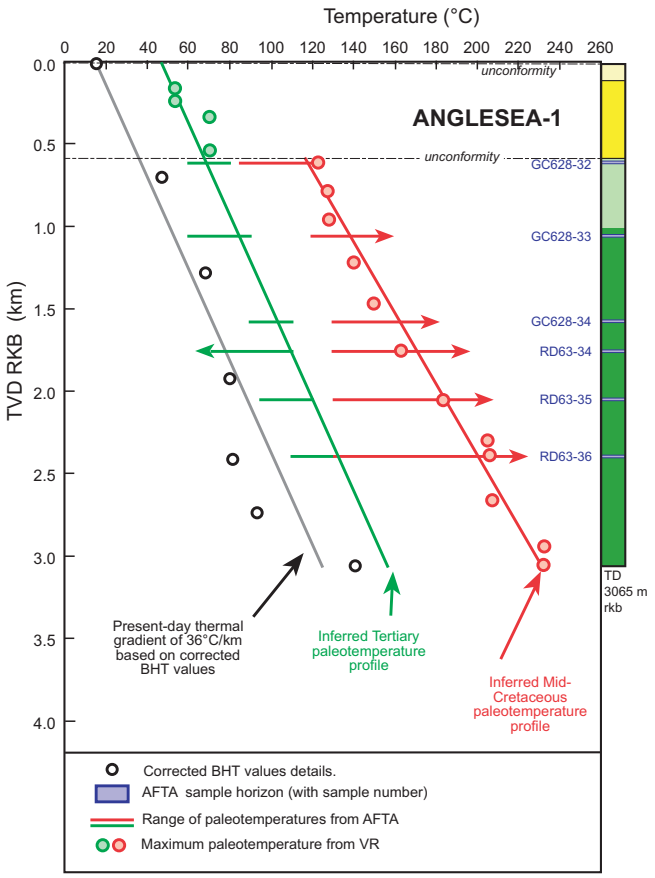

Figure 6. Palaeotemperature constraints from AFTA and VR data in the Anglesea-1 well, plotted against depth, and attributed to one of two paleo-thermal episodes as explained in the text. Tertiary constraints define a linear depth profile, sub-parallel to the present-day temperature profile (derived from corrected BHT values), and offset to higher temperatures by approximately 30 to 40ºC. This suggests that heating was due primarily to deeper burial, with little or no difference in heat flow compared to the present day. In contrast, whilst mid-Cretaceous paleotemperature constraints also define a linear profile, the slope of the profile is distinctly higher that that of the Tertiary paleotemperature profile and the present-day temperature profile, suggesting that a major component of heating in this episode was due to elevated basal heat flow.

Paleogeothermal gradients and removed section

Figure 7 shows the range of values of palaeogeothermal gradient and missing section which are consistent with the palaeotemperature constraints for the Tertiary and mid-Cretaceous paleo-thermal episodes shown in Figure 6. More details of the methods employed in constructing these Figures are provided e.g. by Bray et al. (1992) and Green et al. (2002). Statistical analysis—based on likelihood theory, which is particularly applicable to the ranges of paleotemperature allowed by AFTA data—provides definition of the range of each parameter allowed by the paleotemperature constraints within 95% confidence limits. The two parameters are highly correlated, such that higher paleogeothermal gradients require correspondingly lower values of removed section, and vice versa. This analysis depends on the assumption that the paleogeothermal gradient was linear and can be extrapolated through the removed section to the paleo-surface temperature. Consistency of results in a variety of different settings suggests that this assumption should be valid (Green et al. 1995, 2002). The validity of the results also depends critically on the assumed paleo-surface temperature. We have used a constant value equal to the present-day value of 15ºC for both episodes. If the

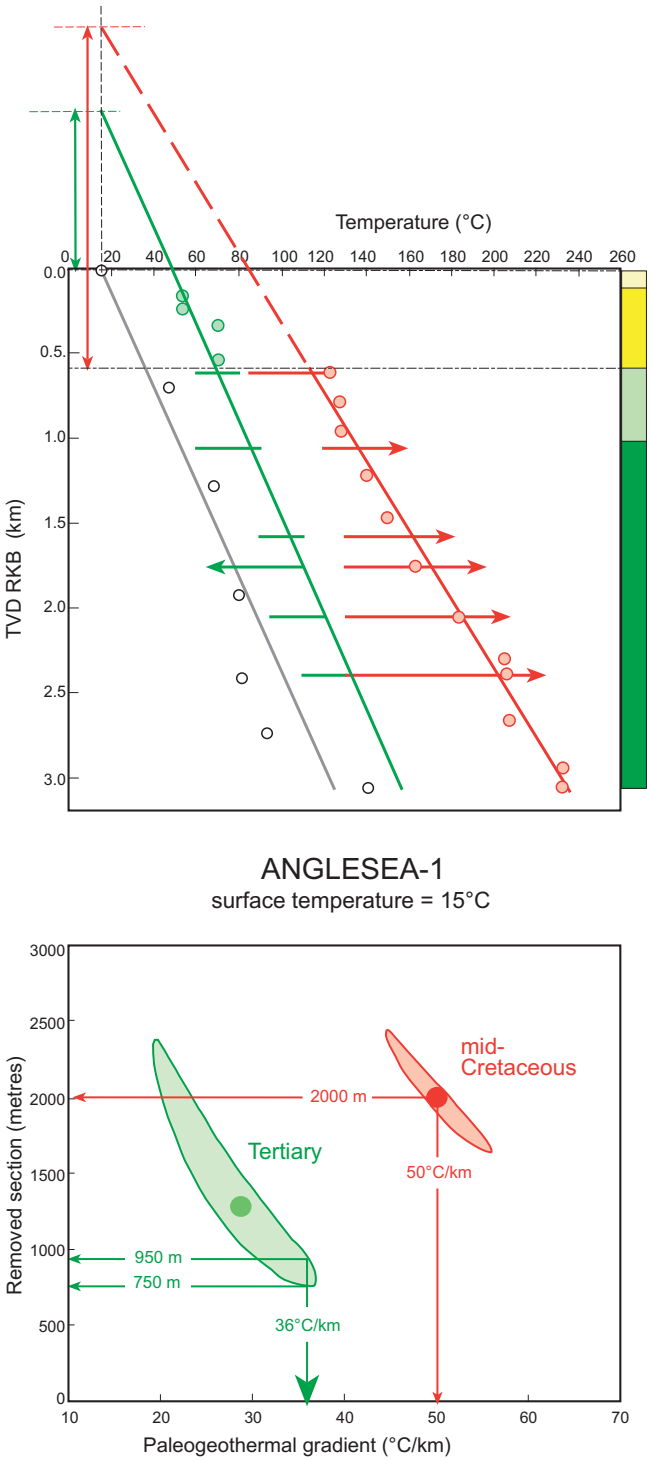

Figure 7. Fitting a linear palaeotemperature profile to the constraints for each episode derived from AFTA and VR data as a function of depth (Fig. 6) and extrapolation to an assumed palaeo-surface temperature of 15ºC allows estimation of the range of palaeogeothermal gradients and removed section that are consistent with the data within 95% confidence limits. Results of this analysis are shown by the shaded zones representing the mid-Cretaceous and Tertiary paleo-thermal episodes identified in the Anglesea-1 well. This approach is based on a number of assumptions, but generally gives results that are consistent with independent evidence, as explained in greater detail by Bray et al. (1992), Green et al. (2002) and Green (2004).

paleo-surface temperature was higher during either event, the amounts of removed section can be easily adjusted by subtracting an amount given by dividing the change in surface temperature by the appropriate value of paleogeothermal gradient.

As shown in Figure 7, the entire range of palaeogeothermal gradients consistent with the mid-Cretaceous paleotemperature constraints is higher than the present-day gradient of 36ºC/km, showing that heating to these paleotemperatures must have been due, at least in part, to elevated heat flow. The best-fit paleogeothermal gradient is very close to 50ºC/km, corresponding to approximately 2 km of additional burial on the Cretaceous-Early Tertiary unconformity in this well. In contrast, the range of paleogeothermal gradients characterising the Tertiary paleo-thermal episode in Figure 7 is mostly lower than the present-day value of 36ºC/km, which is close to the upper end of the allowed range. Thus, the Tertiary paleo-thermal episode can be explained solely in terms of heating due to deeper burial, and allow little or no increase in heat flow during this episode compared to the present-day value. Assuming that the paleogeothermal gradient during the Tertiary episode was the same as the present value, deeper burial by between 750 m and 950 m of additional section—subsequently removed during Late Tertiary uplift and erosion—is required to explain the data.

Thermal and burial/exhumation history reconstruction

Figure 8 illustrates the preferred thermal history reconstruction and the associated burial/exhumation history for the sedimentary units intersected in the Anglesea-1 well, based on the AFTA and VR data discussed so far. These histories are essentially the combination of the Default History discussed earlier with the two events identified on the basis of AFTA and VR data. Cooling in the earlier event is shown as beginning at 95 Ma, although any time between 90 and 100 Ma is allowed. Similarly, cooling in the more recent episode is shown beginning at 10 Ma, but based on the AFTA constraints in Table 1, any time between 55 and 5 Ma is possible (while stratigraphic constraints, assuming that heating was due to deeper burial, show that cooling must have begun later than 35 Ma, as above).

A paleogeothermal gradient of 50ºC/km has been used during the earlier episode (Fig. 7), decreasing to a value equal to the present-day value of 36ºC/km between 90 and 80 Ma, and constant at 36ºC/km since 80 Ma. A total thickness of 2 km of additional mid-to Late Cretaceous section has been deposited between 110 and 95 Ma, and removed during exhumation between 95 and 75 Ma, at which time deposition of the preserved Eastern View Formation began. An additional 850 m of Oligocene to mid-Miocene section is deposited between 35 and 10 Ma and removed during exhumation between 10 and 0 Ma. This scenario is consistent with all aspects of the AFTA and VR data presented in previous sections, but it should be stressed that a range of alternative paleo-gradient scenarios would be allowed by the data in both episodes (Fig. 7). However, due to the constraints provided by the data, if specified values of paleo-gradient within the allowed range for each episode are combined with the appropriate values of removed section, the resulting alternative thermal history reconstructions will be very similar to those shown in Figure 8.

On this basis, the reconstruction is well-constrained by the thermal history constraints obtained from AFTA and VR data in this well in terms of both the magnitude and timing of paleo-thermal effects, as discussed in previous Sections, and should provide a reliable basis for predicting patterns of (U-Th)/He ages with depth to compare with the measured ages.

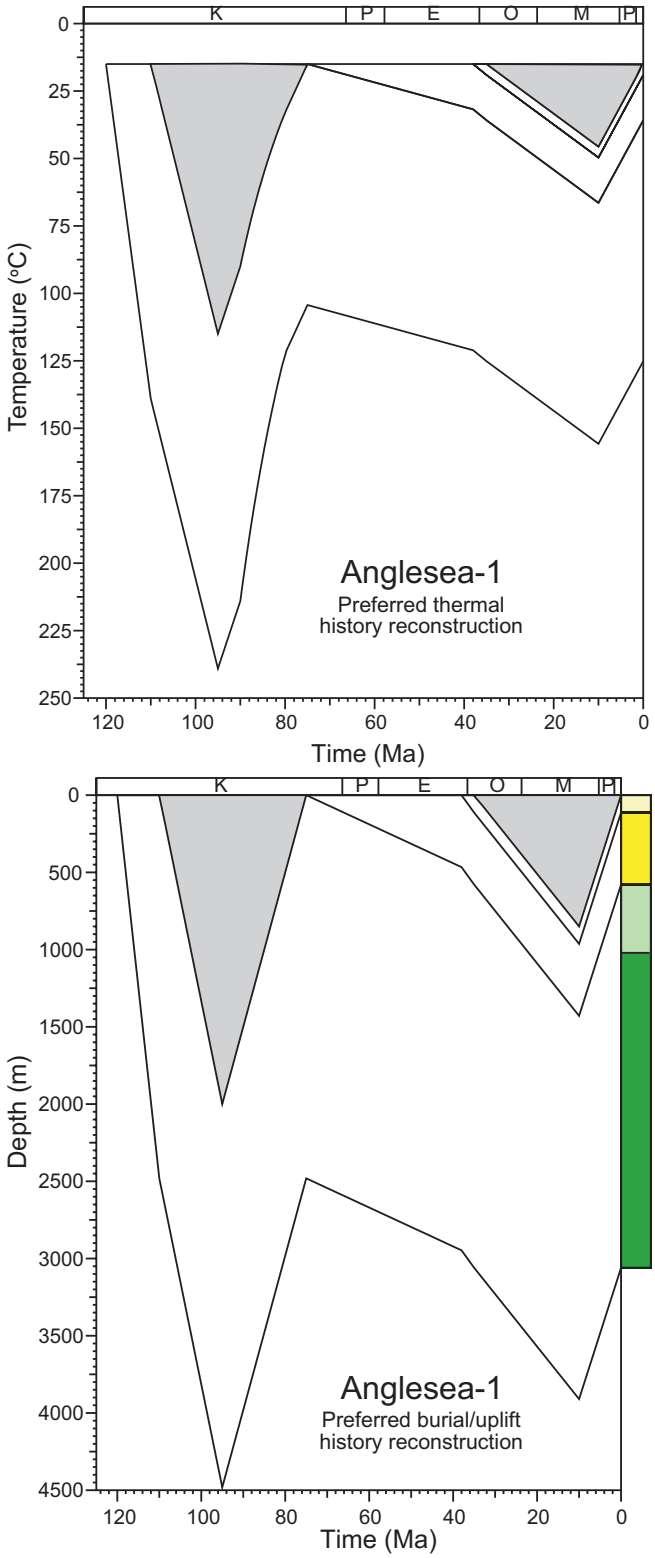

Figure 8. Schematic illustration of the reconstructed thermal and burial/exhumation histories for the Anglesea-1 well, derived from AFTA and VR data discussed here.

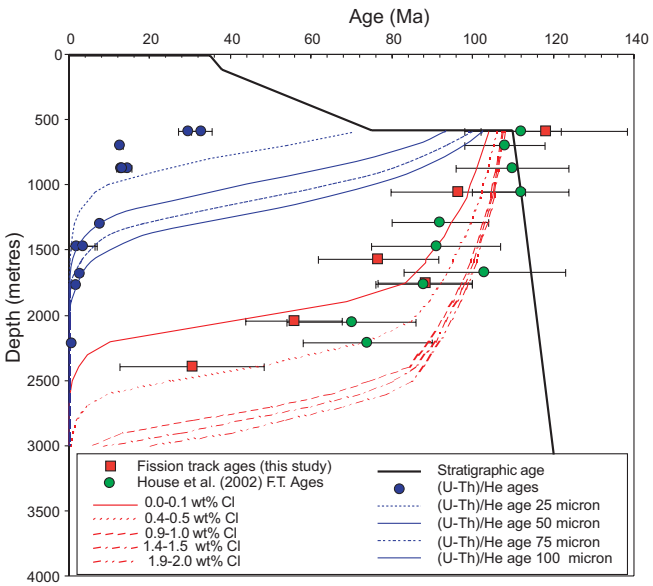

Figure 9. Measured (U-Th)/He ages in samples from Anglesea-1 from House et al. (1999), plus apatite fission track ages from this study (Table 1) and from House et al. (2002), plotted against depth. Trends of (U-Th)/He age vs depth predicted from the "Default Thermal History" scenario (see text) are also plotted, for four values of mean grain radius. Similar trends of fission track age are plotted for five apatite compositions.

Refining the thermal history framework using apatite (U-Th)/He ages

Apatite (U-Th)/He age data

Apatite (U-Th)/He ages in eight samples (including some replicate analyses) from the Early Cretaceous section in Anglesea-1 were reported by House et al. (1999). These ages are plotted against depth in Figure 9, together with the apatite fission track ages measured in this study (Table 1) and those reported by House et al. (2002). Figure 9 illustrates the greater thermal sensitivity of the (U-Th)/He system with respect to fission tracks in apatite, with the (U-Th)/He ages being reduced to close to zero at depths around 2 km where the fission track ages show only minor reduction due to the present-day thermal regime.

Also shown in Figure 9 are trends of (U-Th)/He age with depth, for four different values of grain radius, predicted from the Default Thermal History scenario as outlined earlier, using the He diffusion systematics outlined by Farley (2000). Mean mass-weighted grain radii for apatites from these samples are between 33 and 82 microns (House et al. 2002), so the 25, 50, 75 and 100 micron trends span the relevant range for comparison with the measured data in Figure 9. Similar trends of fission track age versus depth for apatites of different chlorine contents are also shown, for reference.

Two key points immediately emerge from Figure 9. First, the reduction of measured (U-Th)/He age towards zero at depths around 1,500 m to 2,000 m coincides closely with the depth—and therefore temperature—range over which the predicted trends also tend towards zero. This suggests that the overall He diffusion behaviour of these apatites is similar to that embodied in the predictive algorithms employed to model the system (Farley 2000), and therefore that these systematics can be used with confidence to extract information on the paleo-thermal history. Secondly, because many of the measured ages are from the depth/temperature range where the ages decrease rapidly towards zero, only samples from the three shallowest depths are likely to retain any information on the paleo-thermal history, while data in all the deeper samples are effectively dominated by the present-day thermal regime. While this limits the amount of information that can be obtained from the (U-Th)/He ages, it does have the benefit of showing that the interpretive scheme and the present-day thermal regime are consistent.

Since the work of House et al. (1999, 2002), technical improvements in (U-Th)/He thermochronology have led to the capability of analysing single grains of apatite, using a laser-based system to outgas He from the apatite grains, as distinct from the furnace-based system employed by House et al. (1999, 2002). This has the benefit of providing more control on variation in analyses from individual samples, which can be particularly important if grains have been derived from different sediment source terrains. For Otway Group sediments, this is not such a problem, as the great majority of grains share a common volcanic source. In addition, in the case of samples from Anglesea-1, all grains should have been totally outgassed during the earlier of the two post-depositional paleo-thermal episodes identified from AFTA (above). But nevertheless, single grain analyses are desirable for detailed analysis of data, particularly from sedimentary basins.

The original aim of this study was to supplement the data from House et al. (1999) with new single grain data, but the unavailability of equipment has precluded any new analyses. Refining the thermal history reconstruction shown in Figure 8 has therefore been carried out using only the multiple-grain analyses reported by House et al. (1999).

Modelling (U-Th)/He ages in different thermal history scenarios

Measured apatite (U-Th)/He ages represent a balance between production of He from alpha decay of uranium and thorium isotopes, and the temperature-dependent diffusive loss of helium throughout the history of the apatite grains. Thus, in detrital apatite grains from sedimentary rocks, the measured ages have very little meaning in their own right, but reflect the integrated thermal history of the host sample—possibly coupled with the history of sediment source terrains, although as explained above, in the case of the samples from Anglesea-1, this is not important. Therefore, in order to extract information on the magnitude of post-depositional heating from such data, it is necessary to numerically model the He production and diffusion system in apatite, to predict the (U-Th)/He age that is expected from a particular thermal history, and then to compare the predicted ages with measured values—as a function of grain radius if results from multiple grains or sub-samples are available—in order to define the range of scenarios that match the measured ages.

This process is similar, in principle, to that by which thermal history constraints are derived from AFTA data (above). But AFTA data have the advantage that the track length distribution, in addition to the measured fission track age, provides additional constraints on the range of viable histories—the variation of these parameters with chlorine content provides further useful constraints—which allows specific estimates of the maximum paleotemperature and the onset of cooling to be derived for individual samples. In contrast, since the (U-Th)/He age system provides only a measured age, there is a wide range of conditions of maximum temperature and onset of cooling which can produce the same degree of age reduction, and results from individual samples cannot provide specific estimates of these parameters. Modelling the variation of (U-Th)/He age within a vertical sequence provides tighter constraints where data are available over a range of depths or elevations (Wolf et al. 1998). In addition, the within-sample variation of (U-Th)/He age with grain radius also has the potential to provide tighter constraints on the history of

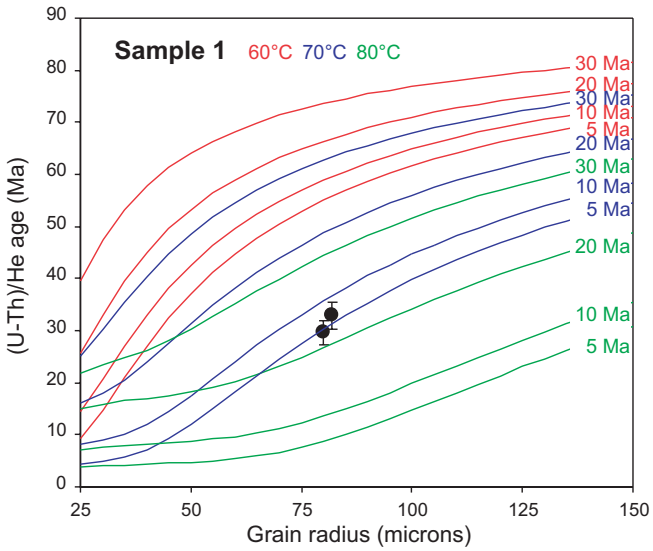

Figure 10. Trends of (U-Th)/He age vs grain radius for sample 1 of House et al. (1999) predicted for various thermal history scenarios within the range of conditions allowed by AFTA data in sample GC628–32 (from the same depth). Measured (U-Th)/He ages in sample 1 are also shown. Only a restricted range of conditions gives predictions that are consistent with both the AFTA and the (U-Th)/He data.

individual sample (Reiners & Farley 2001), if such data are available. But for this study, multiple analyses in individual samples are restricted and this is not possible.

For this reason, to extract thermal history information from the (U-Th)/He ages from Anglesea-1, we have used the thermal history framework established from the AFTA and VR data as a basis, and then investigated how this can be refined using the (U-Th)/He data. In this way, the inherently greater precision of the (U-Th)/He technique can be used to best advantage. Using the variation of temperature with time predicted for each sample from the reconstruction shown in Figure 8, we have modelled the expected (U-Th)/He age as a function of grain radius, and compared the resulting trend with measured ages from each sample. By varying the peak paleotemperature during the more recent paleo-thermal event identified from AFTA and VR, it is then possible to define the range of conditions that give predictions that are consistent with the measured (U-Th)/He ages.

Figure 10 shows results of this procedure in the shallowest of the samples for which apatite (U-Th)/He ages were reported by House et al. (1999), from a depth of 592 m which is the same depth as that from which AFTA sample GC628–32 was taken. AFTA data from sample GC628–32 suggest that the sample began to cool from a peak paleotemperature between 60 and 80ºC some time between 55 and 5 Ma (Table 1). As summarised earlier, stratigraphic constraints further refine the onset of cooling to the interval 35 to 5 Ma. Therefore in Figure 10 predicted trends of (U-Th)/He age vs grain radius are shown for histories involving cooling from a peak paleotemperature of 60ºC, 70ºC and 80ºC at 30 Ma, 20 Ma, 10 Ma and 5 Ma, spanning the range of conditions allowed by AFTA. Clearly, only a limited range of conditions gives predictions that are consistent with the measured (U-Th)/He ages in this sample, which are also plotted in Figure 10 at the appropriate values of mean grain radius. The predicted trend for cooling from 70ºC at 5 Ma agrees very closely with the measured ages, while those corresponding to cooling from 80ºC beginning at 30 and 20 Ma bracket the measured ages. None of the trends corresponding to cooling from a peak of 60ºC match the measured ages.

Figure 11 shows an alternative way of looking at this process, in which conditions—peak paleotemperature and the time at which cooling began—that give predictions which match the measured

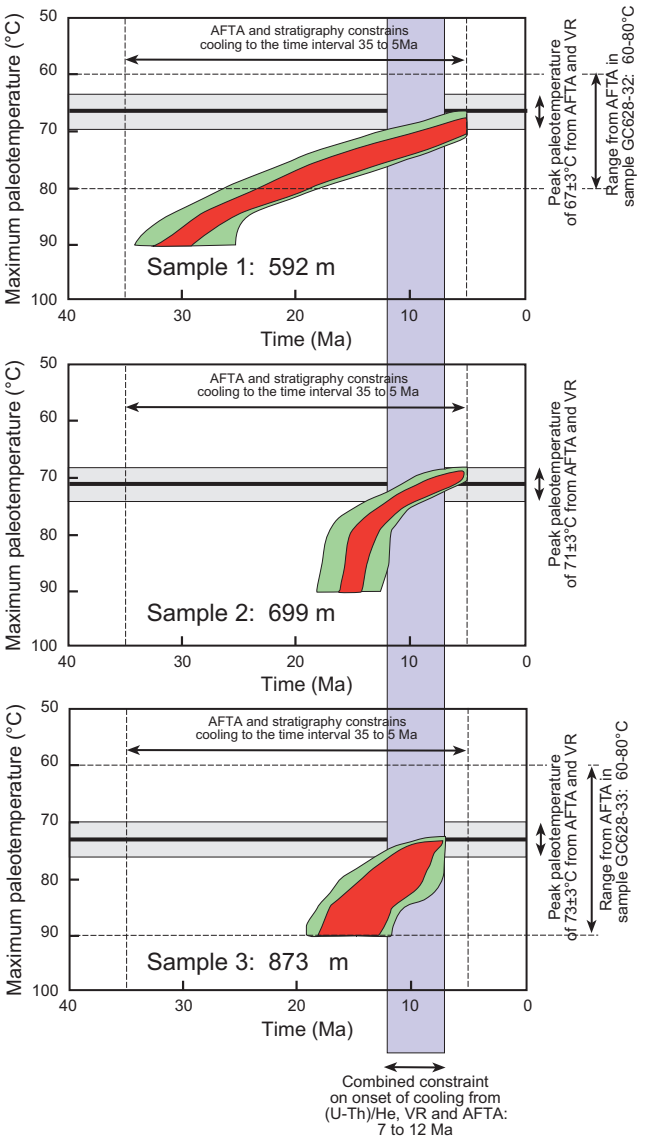

Figure 11. For samples 1, 2 and 3 from House et al. (1999), modelling the (U-Th)/He age expected from a variety of thermal history scenarios allows definition of the range of conditions which give predictions that are consistent with measured ages, as in Figure 10. In these plots, the range of conditions (peak paleotemperature and the time at which cooling began) for which predicted age match the measured ages within analytical uncertainties are shown in red, while conditions for which the predicted values are within 20% of the measured values are shown in green. Horizontal black lines in each plot show the peak Tertiary paleotemperature defined from the preferred thermal history reconstruction illustrated in Figure 8, while the grey zones around these lines correspond to a ±4°C uncertainty around that value, equivalent to the ±100 metre uncertainty in removed section in Figure 7. Conditions allowed by the (U-Th)/He data overlap with those from AFTA and VR only for cooling beginning within the interval 12 to 7 Ma.

ages within the analytical uncertainties are shown in red. To allow the possibility of a wider uncertainty margin, conditions that give predictions within 20% of the measured ages are shown in green. This plot emphasises how a wide range of conditions can predict the same (U-Th)/He age, and the requirement for additional information in order to provide useful thermal history constraints from (U-Th)/He data in a single sample.

Figure 11 also shows the results of similar modelling for (U-Th)/He data from samples at depths of 699 m and 873 m (samples 2 and 3 of House et al. 1999). An upper limit of 90ºC has been used in these plots, as AFTA data from sample GC628–33 (1,057 m

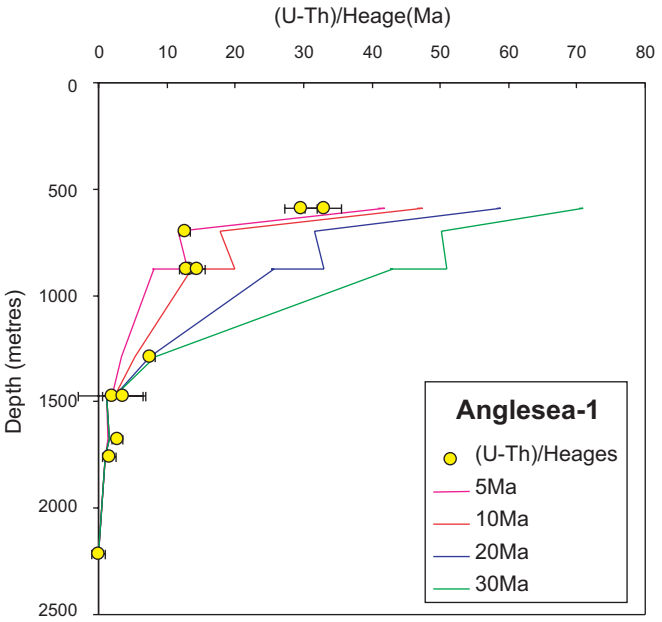

Figure 12. Trends of (U-Th)/He age vs depth predicted from thermal history reconstructions similar to that shown in Figure 8, for cooling beginning at 5 Ma, 10 Ma, 20 Ma and 30 Ma. Later cooling clearly gives the closest match between predicted and measured ages. The slight mismatch in the shallowest sample probably reflects the sensitivity of predicted ages to slight differences in temperature in this range and a slightly higher temperature (within the range allowed by the AFTA and VR data) would improve the match considerably (Fig. 11).

depth) shows that the peak paleotemperature cannot have been greater than this value. For sample 2, only a single (U-Th)/He age was determined by House et al. (1999), but for sample 3, ages were determined in three splits of grains. For coding the conditions according to the agreement between measured and predicted ages in this sample in Figure 11, red colour has been used for conditions which give consistent predictions (within analytical uncertainties) in any one of the three splits, and similarly (within 20%) for green.

The ranges of conditions for which predicted (U-Th)/He ages are consistent with the measured ages in the three samples in Figure 10 overlap with the range of temperatures for each sample horizon for the reconstruction shown in Figure 8 only for cooling beginning some time between 12 and 7 Ma. (Note that we have associated a ±4ºC uncertainty range with the best-fit paleotemperature, to represent the degree of fit to the paleotemperature constraints in Figure 6, corresponding to the ±100 metre uncertainty in the amount of removed section in Fig. 7). Thus, the integrated AFTA, VR and (U-Th)/He dataset in this well are all consistent with thermal and burial/exhumation histories similar to those in Figure 8, provided that cooling in the most recent episode began some time in the Late Miocene, between 12 and 7 Ma.

To illustrate this further, Figure 12 shows the (U-Th)/He ages from House et al. (1999) plotted against depth, together with ages versus depth predicted for thermal history scenarios similar to those in Figure 8, for cooling beginning at 5 Ma, 10 Ma, 20 Ma and 30 Ma. For each case, the degree of heating is based on the mid-point of the range of removed section (850 m) corresponding to a paleogeothermal gradient of 36ºC from Figure 7. The horizontal black lines in Figure 11 also correspond to this condition. Clearly the trends for more recent cooling show the best agreement with the measured ages in Figure 12, although some systematic differences remain, particularly for sample 1, in which the measured ages are younger than predicted for all values of timing. But note that in Figure 11 the range of conditions giving consistent predictions and measured ages for sample 1 do not actually overlap directly with the best-fit paleotemperature from AFTA and VR, which is another manifestation of the slight mismatch in Figure 12.

Note the convergence of all four trends in Figure 12 at depths around 1,200 m and deeper. This emphasises earlier comments reflecting the dominance of the present-day thermal regime at such depths and temperatures, and further illustrates the fact that only the shallower (U-Th)/He ages provide any information on the nature of paleo-thermal effects.

Given that the match between the measured and predicted ages with depth is not perfect (Fig. 12), it is possible that the single Tertiary cooling episode scenario employed in the modelling may not be appropriate. Crowhurst et al. (2002) showed how, by varying the nature of the cooling history, it is possible to obtain a better match with measured (U-Th)/He ages as a function of depth. However, given the nature of the (U-Th)/He dataset available here, with data only on multiple grain splits, and only three samples effectively providing control on the paleo-thermal history, this procedure is not considered to be worth pursuing at this stage. But when single grain age data become available, including more samples from shallower depths, such an approach may indeed allow further refinement of the nature of the Late Tertiary cooling history.

Summary of paleo-thermal episodes and benefits of integrating multiple techniques

Integration of AFTA, VR and (U-Th)/He data from the Anglesea-1 well has resulted in definition of two dominant paleo-thermal episodes with relatively high precision. AFTA and VR data reveal an earlier episode, in which Early Cretaceous units began to cool from maximum post-depositional paleotemperatures some time between 100 and 90 Ma. The mid-Cretaceous paleogeothermal gradient was clearly higher than the present-day value, implying that heating in this episode was due to elevated basal heat flow, coupled with deeper burial by around 2 km of additional Early Cretaceous section (Fig. 7), subsequently removed during mid-Cretaceous exhumation. This episode, thought to be related to initial rifting of the southern continental margin of Australia from Antarctica, has been well documented in a variety of earlier studies (e.g. Duddy 1994, 1997; Cooper 1995; Cooper & Hill 1997), and will not be discussed in detail.

Here, we focus on the more recent episode, also revealed by AFTA and VR data, but defined with greater precision by integration of (U-Th)/He to have begun some time within the interval 12 to 7 Ma. Paleotemperature constraints characterising this episode do not allow paleogeothermal gradients much in excess of the present-day value of 36ºC/km, emphasising that heating and cooling in this episode were due almost entirely to deeper burial and subsequent exhumation.

These results emphasise the benefits to be gained in such studies from integrating data from multiple techniques. VR data in isolation, while reliably defining the magnitude of maximum paleotemperatures through the section, would provide only broad constraints on the timing of events. The break in maturity across the top-Cretaceous unconformity suggests two major cooling events, but it might alternatively be possible to interpret all of the VR data in terms of a single post-Eocene event characterised by a highly elevated paleogeothermal gradient, and only by integrating these data with AFTA does the true nature of the history become clear. AFTA data on their own would confidently reveal two paleo-thermal episodes, but with only minimum constraints on the maximum paleotemperature in the earlier event in most samples—because of total annealing of all tracks prior to cooling—the true nature of the earlier episode would not be clear. Incorporating the VR data reveals the elevated paleogeothermal gradients during this

episode, as well as providing corroborative support for the earlier episode, evidence for which is slightly equivocal in some of the AFTA samples because cooling began so soon after deposition of these units. On their own, (U-Th)/He data would provide only limited definition of the more recent episode, and would provide no evidence of the earlier episode, as the data are dominated by the effects of the more recent episode. But integration of the (U-Th)/He data with results from AFTA and VR provides enhanced precision on the timing of Tertiary cooling, as already discussed. In summary, only by integrating data from all three techniques can both events be defined with confidence.

Integration with regional geology

The effects of Late Tertiary tectonism have been recognised in previous studies of the Eastern Otway Basin. Evidence from hydrocarbon exploration programs in the offshore Torquay Embayment, to the east of the Anglesea-1 well (Fig. 1), as well as the onshore eastern Otway Basin, has revealed localised anticlines of Oligocene age (Trupp et al. 1994) and more widespread structures variously attributed to "Miocene" age (Trupp et al. 1994), "Miocene to Recent" (Cooper 1995) or "Mio-Pliocene" (Cooper & Hill 1997). Cooper & Hill (1997) also highlighted previous reports of a mid-Eocene unconformity offshore.

More recently, Dickinson et al. (2001, 2002) documented the widespread occurrence of a Late Miocene to Pliocene unconformity across much of SE Australia. They interpreted this as representing an interval of significant regional uplift and associated erosion, with maximum effect centred on the present-day Otway Ranges (Fig. 1) where they suggested up to a kilometre of section may have been removed. By defining locations where the erosive effect is minimal, they bracketed the timing of the erosional event to within the interval 10 to 5 Ma, from the depositional age of the youngest and oldest section preserved below and above the unconformity surface.

Results from the Anglesea-1 well presented here are consistent with the regional geological information reviewed by Dickinson et al. (2001, 2002). The refined estimate of the onset of cooling in the Anglesea-1 well, between 12 and 7 Ma, derived from integrating (U-Th)/He data with AFTA, overlaps with the younger part of the range of 10 to 5 Ma for the timing of erosion inferred from geological evidence, and combining both lines of evidence suggests that the best estimate for the onset of erosion (i.e. exhumation) is between 10 and 7 Ma. In addition, the estimate of 750 m to 950 m for the amount of section removed during the Late Miocene exhumation episode in Anglesea-1 (Fig. 7) is highly consistent with the evidence reported by Dickinson et al. (2001, 2002) for the former presence of more than 600 m of Eocene to Middle Miocene units in the region of the present-day Otway Ranges, removed during Late Miocene erosion and exhumation.

Dickinson et al. (2001, 2002) also emphasised the synchroneity between the timing of Late Miocene uplift and erosion in SE Australia with events on a more regional scale, from New Zealand to Papua New Guinea. This is supported by the recent study of the Fresne-1 well, located in the Taranaki Basin (NZ), in which Crowhurst et al. (2002) reported that AFTA dates the onset of inversion to the interval 9 to 8 Ma (while integrating apatite (U-Th)/He ages with the AFTA data also suggests a discrete later episode of inversion). The timing of this inversion phase correlates closely with the inferred timing of 10 to 7 Ma for the onset of exhumation in SE Australia, derived from the combination of thermochronologic and stratigraphic evidence.

Late Miocene exhumation in SE Australia therefore appears to be a truly regional process, probably reflecting a local manifestation of plate-scale processes. Dickinson et al. (2002) also highlighted this aspect, suggesting an origin as a result of a change in plate dynamics in the Late Miocene. A temporal link between events at plate margins and episodes of regional exhumation identified from AFTA in various parts of the world has also been highlighted by Green et al. (2002), and evidence for regional synchroneity and plate-scale driving processes now seems indisputable. Nevertheless, the origin of such processes remains uncertain at present, and further effort is required in this direction in order to understand the underlying driving mechanisms.

Implications for hydrocarbon exploration

The lack of exploration success to date in the offshore Torquay Sub-Basin has been attributed in large part to wells targeting structures formed during Miocene inversion, which most likely post-date the main episode of hydrocarbon generation (e.g. Trupp et al. 1994). The results of this study, and the regional geological evidence discussed above, emphasise that similar problems are likely to beset exploration across most of the Eastern Otway Basin, where the combined effects of elevated heat flow and deeper burial during the mid-Cretaceous led to generation of hydrocarbons from source rocks within the Early Cretaceous section prior to the onset of mid-Cretaceous uplift and erosion and decline in heat flow. After that time, across most of the Eastern Otway Basin, Early Cretaceous source rocks have not been reheated to paleotemperatures in excess of those reached during the mid-Cretaceous paleo-thermal maximum, with the result that no further generation of hydrocarbons from these units has occurred.

In the light of these comments, the restriction of commercial hydrocarbon accumulations in the Eastern Otway Basin to the Port Campbell Embayment and Shipwreck Trough (Tickell et al. 1992; Geary et al. 2001) appears highly significant, as only in this region have the effects of Late Miocene inversion and/or regional exhumation been sufficiently minor that deposition has proceeded more or less continuously throughout Late Cretaceous and Tertiary times, allowing hydrocarbons generated from Early Cretaceous source rocks during Tertiary burial to be trapped in the Late Cretaceous Warre Sandstone (Duddy 1997). Because of the highly restricted region where these conditions pertain, risks associated with hydrocarbon exploration outside this region must be considered extremely high.

Success in future exploration programs in the region pursuing plays involving Early Cretaceous source rocks will require focus either on identifying regions where the effects of Tertiary burial have overcome the influence of earlier paleo-thermal effects and caused significant hydrocarbon generation in more recent times (Duddy 1997), or on the search for early-formed structures which were extant during the main phase of hydrocarbon generation prior to mid-Cretaceous cooling, and have subsequently remained sealed. Alternatively, plays involving post-Cretaceous source rocks may be viable in areas where Tertiary heating has been sufficiently great, although the issue of the relative timing of generation vs formation of structures will still be a vital control on prospectivity.

In all these cases, the regional nature of Late Miocene exhumation also has implications for exploration in terms of possible remigration of hydrocarbons trapped prior to the onset of exhumation, as well as the effects of phase changes associated with the pressure drop due to exhumation, which can cause breaching of seals and loss of hydrocarbons.

Conclusion

This case study illustrates how integration of (U-Th)/He dating with more conventional techniques (e.g. AFTA, VR) provides increased precision in determining the timing of paleo-thermal episodes involving relatively low peak paleotemperatures, and therefore allows greater precision in thermal history reconstruction. This in turn allows improved definition of the thermal evolution of potential hydrocarbon source rocks. Application of these techniques can significantly reduce exploration risk by focussing on regions where hydrocarbon generation post-dates structuring. This study also illustrates how, whereas application of any one technique in isolation provides only partial definition of the history, an integrated AFTA, VR and (U-Th)/He program, enhanced by the availability of regional geological information, can maximise the detail with which paleo-thermal histories can be defined.

References

ARGENT, J.D., STEWART, S.A., GREEN, P.F. and UNDERHILL, J.R., 2002. Strain partitioning and fault reactivation during basin inversion: constraints from new AFTA and seismic data in the Inner Moray Firth Basin, UK North Sea. Journal of the Geological Society of London, v. 159, 715–729.

BRAY, R.J., GREEN, P.F. and DUDDY, I.R., 1992. Thermal history reconstruction in sedimentary basins using apatite fission track analysis and vitrinite reflectance: a case study from the east Midlands of England and the Southern North Sea. *In:* Hardman, R.F.P. (Ed), Exploration Britain: Into the next decade, Geological Society of London, Special Publication 67, 3–25.

BURNHAM, A.K. and SWEENEY, J.J., 1989. A chemical kinetic model of vitrinite reflectance maturation: Geochimica et Cosmochimica Acta., v. 53, 2,649–2,657.

COOK, A.C. (Ed), 1982. The origin and petrology of organic matter in coals, oil shales and petroleum source rocks: University of Wollongong, Wollongong, New South Wales, 106 p.

COOK, A.C., MURCHISON, D.G. and SCOTT, E., 1972. Optically biaxial anthracitic vitrinites. Fuel, v. 51, 180–184.

COOPER, G.T., 1995. Seismic structure and extensional development of the eastern Otway Basin–Torquay Embayment. APEA Journal, v. 35, 436–450.

COOPER, G.T. and HILL, K.C., 1997. Cross-section balancing and thermochronological analysis of the Mesozoic development of the eastern Otway Basin. APPEA Journal 37, 615–633.

CONSTANTINE, A., LIBERMAN, N., NGUYEN, C. and SMITH, T., 2001. Otway Basin source rock, vitrinite reflectance and reservoir properties CD-ROM. Minerals and Petroleum Victoria, Open File Report.

CROWHURST, P.V., GREEN, P.F. and KAMP, P.J.J., 2002. Appraisal of (U-Th)/He apatite thermochronology as a thermal history tool for hydrocarbon exploration: an example from the Taranaki Basin, New Zealand. American Association of Petroleum Geologists Bulletin, v. 86, 1801–1819.

CROWLEY, P.D., REINERS, P.W., REUTER, J.M. and KAYE, G. D., 2002. Laramide exhumation of the Bighorn Mountains, Wyoming. An apatite (U-Th)/He thermochronology study. Geology, v. 30, 27–30.

DICKINSON, J.A., WALLACE, M.W., HOLDGATE, G.R., DANIELS, J., GALLAGHER, S.J. and THOMAS, L., 2001. Neogene Tectonics in SE Australia: implications for Petroleum Systems. APPEA Journal, v. 41. 37–52.

DICKINSON, J.A., WALLACE, M.W., HOLDGATE, G.R., GALLAGHER, S.J. and THOMAS, L., 2002. Origin and timing of the Miocene-Pliocene unconformity in southeast Australia. Journal of Sedimentary Research, v. 72, 288–303.

DUDDY, I.R., 1994. The Otway Basin: thermal, structural, tectonic and hydrocarbon generation histories. NGMA/PESA Otway Basin Symposium Extended Abstracts 14, 35–42.

DUDDY, I.R., 1997. Focussing exploration in the Otway Basin: understanding timing of source rock maturation. APPEA Journal, v. 37, 178–191.

DUDDY, I.R. and EROUT, B., 2001. AFTA®-calibrated 2-D modelling of hydrocarbon generation and migration using Temispak®: preliminary results from the Otway Basin. *In:* Hill, K.C. and Bernecker, T. (Eds), Eastern Australasian Basins Symposium, A Refocussed Energy Perspective for the Future, Petroleum Exploration Society of Australia, Special Publication, 485–497.

DUDDY, I.R., EROUT, B., GREEN, P.F., CROWHURST, P.V. and BOULT, P.J., 2003. Timing constraints on the structural history of the Western Otway Basin and implications for hydrocarbon prospectivity around the Morum high, South Australia. APPEA Journal, v. 43, 59–83.

DUDDY, I.R., GREEN, P.F. and LASLETT G.M., 1988. Thermal annealing of fission tracks in apatite 3. Variable temperature behaviour. Chemical Geology (Isotope Geoscience Section) 73, 25–38.

DUDDY, I.R., GREEN, P.F., HEGARTY, K.A. and BRAY, R.J., 1991. Reconstruction of thermal history in basin modelling using Apatite Fission Track Analysis: what is really possible. Proceedings of the First Offshore Australia Conference (Melbourne) III–49– III–61.

DUDDY, I.R., GREEN, P.F., BRAY, R.J. and HEGARTY, K. A., 1994. Recognition of the Thermal Effects of Fluid Flow in sedimentary Basins. *In:* Parnell, J. (Ed), Geofluids: Origin, Migration and Evolution of Fluids in Sedimentary Basins, Geological Society of London, Special Publication 78, 325–345.

DUDDY, I.R., GREEN, P.F., HEGARTY, K.A., BRAY, R .J. and O'BRIEN, G.W., 1998. Dating and duration of hot fluid flow events determined using AFTA® and vitrinite reflectance-based thermal history reconstruction. *In:* Parnell, J. (Ed), Dating and duration of fluid flow and fluid-rock interaction, Geological Society of London, Special Publication 144, 41–51.

DUNCAN, W.I., GREEN, P.F. and DUDDY, I.R., 1998. Source rock burial history and seal effectiveness: Key facets to understanding hydrocarbon exploration potential in the East and Central Irish Sea Basins, American Association of Petroleum Geologists Bulletin, v. 82, 1,401–1,415.

FARLEY, K.A., 2000. Helium diffusion from apatite: general behaviour as illustrated by Durango fluorapatite: Journal of Geophysical Research, v. 105 (B2), 2,903–2,914.

FARLEY, K.A., RUSMORE, M.E. and BOGUE, S.W., 2001. Post-10 Ma uplift and exhumation of the North Coast Mountains, British Columbia. Geology, v. 29, 99–102.

GALBRAITH, R.F. and LASLETT, G.M., 1993. Statistical methods for mixed fission track ages: Nuclear Tracks 21, 459–470.

GALLAGHER, K., 1995. Evolving temperature histories from apatite fission-track data. Earth and Planetary Science Letters, v. 136, 421–435.

GEARY, G.C., CONSTANTINE, A.E. and REID, I.S.A., 2001. New perspectives on structural style and petroleum prospectivity, Offshore Eastern Otway Basin. *In:* Hill, K.C. and Bernecker, T. (Eds), Eastern Australasian Basins Symposium, A refocussed Energy Perspective for the Future, Petroleum Exploration Society of Australia, Special Publication, 507–517.

GLEADOW, A.J.W. and DUDDY, I.R., 1981. Fission track analysis: a new tool for the evaluation of thermal histories and hydrocarbon potential. APEA Journal, v. 23, 93–102.

GREEN, P.F., 2002. Early Tertiary palaeo-thermal effects in Northern England: reconciling results from apatite fission track analysis with geological evidence. Tectonophysics, v. 349, 131–144.

GREEN, P.F., 2004. Post-Carboniferous burial and exhumation histories of Carboniferous rocks of the Southern North Sea and adjacent Onshore UK. Proceedings of the Yorkshire Geological Society. In press.

GREEN, P.F., DUDDY, I.R., GLEADOW, A.J.W., TINGATE, P.R. and LASLETT, G.M., 1986. Thermal annealing of fission tracks in apatite 1. A qualitative description: Chemical Geology (Isotope Geoscience Section), v. 59, 237–253.

GREEN, P.F., DUDDY, I.R., GLEADOW, A.J.W. and LOVERING, J.F., 1989a. Apatite Fission Track Analysis as a palaeotemperature indicator for hydrocarbon exploration. *In:* Naeser, N.D. & McCulloh, T. (Eds), Thermal history of sedimentary basins-methods and case histories, Springer-Verlag, New York, 181–195.

GREEN, P.F., I.R. DUDDY, G.M. LASLETT, K.A. HEGARTY, A.J.W. GLEADOW, and J.F. LOVERING, 1989b. Thermal annealing of fission tracks in apatite 4. Quantitative modelling techniques and extension to geological timescales: Chemical Geology (Isotope Geoscience Section), v. 79, 155–182.

GREEN, P.F., DUDDY, I.R. and BRAY, J.R., 1995. Applications of Thermal History Reconstruction in inverted basins. *In:* Buchanan, J.G. and Buchanan, P.G. (Eds), Basin Inversion, Geological Society of London, Special Publication 88, 149–165.

GREEN, P.F., DUDDY, I.R. and BRAY, R.J., 1997. Variation in thermal history styles around the Irish Sea and adjacent areas: implications for hydrocarbon occurrence and tectonic evolution. *In:* Meadows, N.S., Trueblood, S., Hardman, M. and Cowan, G. (Eds), Petroleum Geology of the Irish Sea and Adjacent Areas, Geological Society of London, Special Publication 124, 73–93.

GREEN, P.F., DUDDY, I.R., BRAY, R.J, DUNCAN, W.I. and CORCORAN, D., 2001a. Thermal history reconstruction in the Central Irish Sea Basin. *In:* Shannon, P.M., Haughton, P.M. and Corcoran, D. (Eds), Petroleum Exploration of Irelands Offshore Basins. Geological Society of London, Special Publication 188, 171–188.

GREEN, P.F., HEGARTY, K.A. and DUDDY, I.R., 1996. Compositional influences on fission track annealing in apatite and improvement in routine application of AFTA®. AAPG, San Diego, Abstracts with Program, p. A.56.

GREEN, P.F., J.D HUDSON, and THOMSON, K., 2001b. Recognition of tectonic events in undeformed regions: contrasting results from the Midland Platform and East Midlands Shelf, Central England. Journal of the Geological Society of London, v. 158, 59–73.

GREEN, P.F., DUDDY, I.R and HEGARTY, K.A., 2002. Quantifying exhumation from apatite fission-track analysis and vitrinite reflectance data: precision, accuracy and latest results from the Atlantic margin of NW Europe. *In:* Doré, A.G., Cartwright, J., Stoker, M.S., Turner, J.P. and White, N. Exhumation of the North Atlantic Margin: Timing, mechanisms and Implications for Petroleum Exploration. Geological Society of London, Special Publication 196, 331–354.

HARLAND, W.B., ARMSTRONG, R.L., COX, A.V., CRAIG, L.E., SMITH, A.G. and SMITH, D.G., 1989. A geologic time scale. Cambridge University Press.

HOUSE, M.A., B.P. WERNICKE, K.A. FARLEY, and DUMITRU, T.A., 1997. Cenozoic thermal evolution of the central Sierra Nevada, California, from (U-Th)/He thermochronometry, Earth and Planetary Science Letters, v. 151, 167–179.

HOUSE, M.A., FARLEY, K.A. and KOHN, B.P., 1999. An empirical test of helium diffusion in apatite, borehole data from the Otway Basin, Australia: Earth and Planetary Science Letters, v. 170, 463–474.

HOUSE, M.A., FARLEY, K.A. and KOHN, B.P., 2002. Evaluating thermal history models for the Otway Basin, southeastern Australia, using (U-Th)/He and fission track data from borehole apatites, Tectonophysics, v. 349, 277–295.

HURFORD, A.J.H. and GREEN, P.F., 1983. The zeta age calibration of fission-track dating, Chemical Geology (Isotope Geoscience Section), v. 1, 285–317.

LASLETT, G.M., GREEN, P.F., DUDDY, I.R. and GLEADOW, A.J.W., 1987. Thermal annealing of fission tracks in apatite 2: A quantitative analysis, Chemical Geology (Isotope Geoscience Section), v. 65, 1–13.

LIPPOLT, H.J., LEITZ, M., WERNICKE, R.S. and HAGEDORN, B., 1994. (Uranium + thorium)/helium dating of apatite: experience with samples from different geochemical environments, Chemical Geology (Isotope Geoscience Section), v. 112, 179–191.

REINERS, P.W. and FARLEY, K.A., 2001. Influence of crystal size on apatite (U-Th)/He thermochronology, an example from the Bighorn Mountains, Wyoming: Earth and Planetary Science Letters 188, 413–420.

SWEENEY, J.J. and BURNHAM, A.K., 1990. Evaluation of a simple model of vitrinite reflectance based on chemical kinetics. American Association of Petroleum Geologists Bulletin, v. 74, 1,559–1,570.

TICKELL, S.J., EDWARDS, J. and ABELE, C., 1992. Port Campbell Embayment 1:100 000 map geological report. Geological Survey of Victoria Reports, 95.

TING, F.T.C., 1978. Petrographic techniques in coal analysis, *In:* KARR, C. (Ed), Analytical methods for coal and coal products, v.1, Orlando, Florida, Academic Press, 3–26.

TISSOT, B.P. and WELTE, D.H., 1984. Petroleum formation and occurrence. Springer-Verlag.

TRUPP, M.A., SPENCE, K.W. and GIDDING, M.J., 1994. Hydrocarbon prospectivity of the Torquay Sub-Basin, Offshore Victoria. APEA Journal, v. 34, 479–494.

WOLF, R.A., K.A. FARLEY, and L.T. SILVER, 1996. Helium diffusion and low-temperature thermochronometry of apatite. Geochimica et Cosmochimica Acta., v. 60, 4,231–4,240.

WOLF, R.A., K.A. FARLEY, and L.T. SILVER, 1997. Assessment of (U-Th)/He thermochronometry: the low temperature history of the San Jacinto mountains, California. Geology, v. 25, 65–68.

WOLF, R.A., FARLEY, K.A. and WOLF, D.M., 1998. Modelling of the temperature sensitivity of the apatite (U-Th)/He thermochronometer. Chemical Geology, v. 148, 105–114.

ZEITLER, P.K., HERCZIG, A.L., MCDOUGALL, I. and HONDA, M., 1987. U-Th-He dating of apatite: A potential thermochronometer: Geochimica et Cosmochimica Acta., v. 51, 2,865–2,868.

ZHANG, E and DAVIS, A., 1993. Coalification patterns of the Pennsylvanian coal measures in the Appalachian foreland basin, western and south-central Pennsylvania. Geological Society of America Bulletin, v. 105, 162–174.